

Application of Evolutionary Algorithms to Flow Control Optimization

Narendra K Beliganur.*
University of Kentucky, Lexington, KY 40506

Dr. Raymond P LeBeau Jr.‡
University of Kentucky, Lexington, KY 40506

Computational Fluid Dynamics (CFD) in conjunction with an evolutionary search algorithm like a genetic algorithm (GA) potentially offers a more efficient and robust optimization method for current flow control designs. As the parameter space under investigation increases in complexity, the performance of evolutionary search algorithms remains high and becomes increasingly effective as compared to gradient-based methods. Based on previous work optimizing a two-jet system using a EARND genetic algorithm, this paper evaluates the performance of a Continuous Genetic Algorithm (CGA) on small arrays of blowing and suction jets on a NACA 0012 airfoil. Results of the four jet control system are discussed and a comparison of the two GA approaches is presented.

Nomenclature

A	= suction or blowing amplitude
A_H	= height of computation area
A_W	= width of computation area
c	= airfoil chord length
C_d	= drag coefficient
C_{dB}	= drag coefficient of baseline (no jet) configuration
C_l	= lift coefficient
C_{lB}	= lift coefficient of baseline (no jet) configuration
i, j	= array, spatial indices
L_j	= location of jet on surface in terms of percent chord
Re	= Reynolds number
x, y	= spatial location
α	= angle of attack
β	= angle between freestream velocity direction and the local airfoil surface
μ	= mean value
σ	= standard deviation
θ	= suction or blowing angle, measured relative to the local airfoil surface

I. Introduction

THE use of evolutionary algorithms (EAs) is now relatively widespread as a tool to optimize complex design spaces. Some recent examples of EAs used in conjunction with computational fluid dynamics (CFD) include the design of airfoils ⁽¹⁾ and turbine cascades ⁽²⁾, but there are numerous other applications. The advantages of an evolutionary algorithm approach should increase as the parameter space becomes increasingly complex, with a growing number of local extrema potentially masking the optimal solution.

The potential for an EA-CFD approach has been demonstrated for a two-jet flow control array using a genetic algorithm ^(3, 4). In these papers, the resulting parameter space has only included 4 or 5 variables regarding the jet

* Graduate Student, Dept. of Mechanical Engineering, 216 Ralph G. Anderson Building, Student Member AIAA

‡ Assistant Professor, Dept. of Mechanical Engineering, 151 Ralph G. Anderson Building, Associate Fellow AIAA

arrangement, with other aspects of the jets as well as the background flow conditions being fixed. A realistic simulation would involve many more possible parameters through investigating more aspects of the jet configuration and the addition of more jets. The inclusion of three-dimensional and unsteady effects (such as synthetic zero-mass jets) will further complicate the picture. Given these possibilities, our immediate focus is on increasing the size of the parameter space through the introduction of more jets, as an assessment of the results can reasonably be made in light of the previous two-jet system outcomes and the earlier single jet work on the same airfoil⁽⁴⁾.

With additional complications, the demands on the GA-CFD system will likewise grow. For example, an increase in genomes and generations might be necessary to achieve satisfactory convergence in a more complex parameter space. Similarly, the addition of more and more complicated jets, unsteadiness, and a third dimension will place much greater demands on the flow solver used to evaluate each genome. While most of these concerns could be address by access to infinite computer power, the authors regrettably do not have such access. As such, the focus of this paper is an evaluation of GA-CFD techniques in the light of assessing the potential for investigating more complicated flow control systems more robustly and efficiently. Application of such a GA-CFD system is presented for four jet simulations and a comparison of two different GA approaches is presented.

II. The GA-CFD System

The GA-CFD system employed for the previous^(3, 4) two-jet studies was a combination of the Explicit Adaptive Range Normal Distribution(EARNND) GA and the GHOST CFD code for purposes of evaluating the fitness of the genomes (through computation of lift and drag coefficients). For the four-jet simulation, along with the EARNND GA, a different GA approach viz. a Continuous Genetic Algorithm (CGA) is also used to evaluate the fitness of the genomes. A brief explanation of the two GA approaches and the CFD code along with the computation platform is presented in the following section. Here, we also explain the general grid setup used for the four-jet simulation.

A. Genetic Algorithms

As mentioned earlier, two different genetic algorithm approaches have been employed in conjunction with the CFD computations. One of the algorithms used in this research is called the “Explicit Adaptive Range Normal Distribution” (EARNND)^(3, 4) genetic algorithm with diversity control. This is a real-coded algorithm in which the corresponding design variables are encoded into a vector of real numbers that is conceptually closest to the real design space. Second, to address the convergence problem, an additional normal distribution scheme is added into the basic GA in order to monitor the global optimization process and balance the workload between the global and local searching process. Moreover, design parameters are explicitly updated to eliminate unnecessary evaluations (computations) in un-promising areas. Finally, diversity control is added to the selection function during the initial part (typically 20%) of the evolution to reduce local early convergence. A general description of this GA may be found here^(3, 4).

A second genetic algorithm approach is a Continuous Genetic Algorithm⁽⁵⁾ which starts with a similar base GA. At each generation, the results are sorted by fitness and the most-fit individuals (typically 25-50% of the total) are selected to continue automatically to the next generation. The remaining individuals of the previous generation are replaced through a mating process using only the most-fit set of individuals. Mutation is then applied to the full generation. This approach tends to accelerate convergence, but does reduce the diversity of covered parameter space. This approach also can potentially reduce the number of simulations required since individuals that are carried unmodified from generation to generation do not have to be recalculated.

The current implementation of the genetic algorithm is designed for commodity clusters or similar architectures but with little modification it may be used on any system. The code is run from a server node on which a specified number of genomes from the current generation are selected, the grids generated, and then the required data is transferred into a series of directories, one corresponding to each genome. These directories are then distributed among the designated set of nodes for the CFD evaluation of a given genome. The CFD computation may be accomplished on a single or multiple processors, depending on the choice of the user. Once the computation is completed, the resultant fitness data is collected by the server node while simulation details not needed for the genetic search process are stored for future reference. Sets of genomes are similarly simulated until the full generation is completed; then, the server node applies the genetic search algorithm to generate a new generation and the process is repeated until the desired full evolution is complete.

B. Computational Platforms

Several computational platforms will be available for these simulations. At the University of Kentucky, three of the Kentucky Fluid Cluster series have been used on GA-CFD simulations: KFC2, KFC4, and KFC5. KFC2 consists of commodity nodes each with a 2000+XP AMD Athlon processor and 256 MB RAM. The network is four-way channel bonded Fast Ethernet. Due to age, KFC2 is now down to 32 stable nodes (from 48 three year ago). KFC4 has also recently been reconfigured into a 47 node system linked by both a single Fast Ethernet switch network and a single Gigabit switch network. Each node has 512 MB RAM and a 2500+ AMD Athlon Barton processor. The third cluster used is KFC5, which has 47 nodes on a single Gigabit switch, with a processing element of a 3200+ AMD Athlon 64 processor (939 pin), 512 KB L2 cache, and 512 MB main memory on each node.

C. CFD Code

Previous and current computations of the multi-jet problem were performed with the CFD code, GHOST. GHOST is an in-house CFD code originally developed at the University of Kentucky by Dr. P. G. Huang. The code is based on a finite volume structured formulation with chimera overset grids. The QUICK and TVD schemes are applied to discretize the convective terms in the momentum and turbulence equations, respectively; the central difference scheme is used for the diffusive terms and the second order upwind time discretization is employed for the temporal terms. This code has been tested extensively and is routinely used for turbulence model validation and 2D flow control analysis^(5, 7). The code employs a variety of Reynolds-Averaged Navier Stokes Turbulence models and Menter SST two equation model is used in this case. The multi-block and chimera features of the code allow the use of fine grid patches near the jet entrance and in regions of highly active flow. The code also employs MPI parallelization to allow different computational zones to be solved on multiple processors. Simulations have been performed on a variety of computer architectures as discussed above.

D. Flow Geometry and Grid Construction

The flow under consideration is that on a NACA 0012 at an 18 degree angle-of-attack and a Reynolds number of 500,000. The basic two-dimensional grid consists of 11 background blocks in a three-by-three pattern, the central region consisting of three subgrids over which the airfoil grid is placed (Fig.1). The airfoil grid is decomposed into 5 subgrids (Fig.2). The grid density on the top portion of the airfoil where the jets are typically placed (i.e. from 5% of chord length to 80% of chord length) is made equal to the density of the jets. With this kind of a grid setup we can quite easily place the suction and blowing jets along the available length by simply varying the boundary conditions at the required point. Also, we can increase or decrease the number of jets or move towards an array of jets, as this no longer requires any change in grid generation. The dimensionless outer boundary of the computational area is chosen as $A_H \times A_W = 8c \times 12c = 8.0 \times 12.0$, large enough to prevent the outer boundary from significantly affecting the near flow field around the airfoil.

On the outer boundary, the left (inlet) boundary is fixed with a uniform dimensionless inlet velocity of unity, the upper and lower boundary condition are “free-stream” boundaries which satisfy the Neumann condition, and the right (outflow) boundary condition is set to a zero velocity gradient condition. For the airfoil blocks, the inner boundary condition is a no-slip wall boundary condition, and the outside boundary is set to “overlap” which allows the background grid points being overlapped by the airfoil block grid points to interpolate values from the foreground airfoil grid points. Computation information between adjacent blocks is exchanged by two ghost points. All the parameters chosen in the computation are dimensionless. The near wall y^+ values of the airfoil blocks were generally kept within 0.5, well within the viscous sublayer region. Details on general grid independence and numerical accuracy for this case without flow control jet have been presented in previous work^(5, 6) and are generally satisfactory for the given grid. For the steady jet array GA-CFD computations, the total number of grid points was 180,000.

Three parameters (Fig. 3) for each jet are selected for the search investigation, namely jet location L_j (measured in percent chord), suction/blowing amplitude A (measured in term of orifice velocity relative to the inflow freestream velocity), and suction/blowing angle θ . The jet width for both suction and blowing is fixed at 2.5% chord length based on a study by Dannenberg⁽⁷⁾, who showed that an increase of suction area beyond 2.5% chord length will not increase lift significantly. In the numerical investigation, the jet entrance velocity is set as

$$\begin{aligned}u &= A \cdot \cos(\theta + \beta) \\v &= A \cdot \sin(\theta + \beta)\end{aligned}$$

where β is the angle between the free-stream velocity direction and the local jet surface, and θ is the angle between the local jet surface and jet entrance velocity direction. Note that a negative θ corresponds to suction while positive indicates blowing. Thus, perpendicular suction is -90° and perpendicular blowing is 90° .

The previous suction-blowing jet studies ^(6, 8) have demonstrated that the potential flow control due to suction tends to be much more significant than that of blowing in this configuration. In order to prevent suction control from dominating the genetic search (and thereby significantly reducing the complexity of the parameter space), the maximum possible flux is split between the two suction jets evenly, with the flux of the first jet fixed at half of the total maximum (0.02121) and the other allowed to vary between zero and 0.02121. The blowing jet amplitude is treated similarly except both jets are allowed to vary between zero and half the maximum flux which in this case is 0.1414.

III. Results of the steady four jet GA-CFD System

A. Four Jet Simulation

A four jet simulation consisting of two suction and two blowing jets has been completed. As compared to the two jet setup, this evolution more than doubles the number of parameters considered. Angle and location for each jet is allowed to vary in the same ranges as the two jet case and the amplitude of one suction jet is fixed as before. The simulation consisted of 50 generations with 56 genomes per generation. Both the GA approaches (viz. EARND and CGA) are used to evaluate the parameter space and the results are compared. In general, the jet parameters for this case were allowed to vary over the following initial ranges:

Suction location -1 (L_{jS1}):	$0.05 \leq L_{jS1} \leq 0.80$	Blowing location -1 (L_{jB1}):	$0.05 \leq L_{jB1} \leq 0.80$
Suction angle - 1 (θ_{S1}):	$-90^\circ \leq \theta_{S1} \leq 0^\circ$	Blowing angle - 1 (θ_{B1}):	$0^\circ \leq \theta_{B1} \leq 90^\circ$
Suction Amplitude - 1 (A_{S1}):	$A_{S1} = 0.02121$	Blowing amplitude - 1 (A_{B1}):	$0.0 \leq A_{B1} \leq 0.1414$
Suction location -2 (L_{jS2}):	$0.05 \leq L_{jS2} \leq 0.80$	Blowing location - 2 (L_{jB2}):	$0.05 \leq L_{jB2} \leq 0.80$
Suction angle - 2 (θ_{S2}):	$-90^\circ \leq \theta_{S2} \leq 0^\circ$	Blowing angle - 2 (θ_{B2}):	$0^\circ \leq \theta_{B2} \leq 90^\circ$
Suction Amplitude - 2 (A_{S2}):	$0.0 \leq A_{S2} \leq 0.02121$	Blowing amplitude - 2 (A_{B2}):	$0.0 \leq A_{B2} \leq 0.1414$

The fitness function used for evaluation of each individual was same for both the GA's.

$$(Fit_A)_{\max} = a \cdot C_l / C_{lB} + b \cdot C_{dB} / C_d$$

a and b were set to 1, providing equal weight to both lift and drag and making the baseline fit equal to 2.0.

Previously ⁽¹³⁾ we have presented some of the results in the context of comparing evolutionary algorithms. Current results of the four jet configurations are augmented with a greater discussion on the effect of the change in jet configuration with regard to the flow physics of the problem. The Continuous GA search evolution achieves a maximum fitness of 2.191 or an improvement of 9.5% over the baseline fitness. Shown in Table 1 is the most fit configuration from the entire evolution to an excessive degree of numerical precision, and Fig.4a and Fig.4b presents all of the configurations sorted by fitness. The configurations that yield the best fitness are those where both suction jets take a leading position (5%-10% chord) on the airfoil, with an orientation approaching normal suction, and both jets operating at near-maximum amplitude. In effect, the two jets act much like a single suction jet. Suction jet 2 is generally the trailing jet and seems to favor a slightly less normal orientation compared to suction jet 1.

For the blowing jets, the best solutions have one blowing jet (typically jet 1) located towards the trailing edge (greater than 65% chord) at a moderate angle (20 deg–40 deg) and at less than the maximum possible amplitude (about 10% the freestream velocity). The second jet is generally located near the middle of the airfoil surface (50% chord) with a lower amplitude (1%-7% freestream) that the more rearward jet and a near-tangential angle. However, there are a considerable number of solutions that violate these general conditions, suggesting that the blowing jet plays a less important role in this flow control scheme, with high results possible even when one of the blowing jets approach zero amplitude. So, like in the previous⁴ two jet studies, the suction jets play the dominant role. In term of the flow field, the lift and drag improvements are related to the collapse of the separation bubble due to the addition of the jets as shown in Fig.5. Fig.5-a show the baseline case where a prominent separation bubble is observed which is considerably reduced in Fig.5-b, which has the jets in optimum configuration space. In figure-6, multiple jet

combinations using the values from the best configuration in Table 1 have been conducted, with the resulting lift and drag coefficients and fitness tabulated in Table 2. In the case of no jets, a prominent separation region is visible (Fig. 6-a). Adding first one and then a second suction jet (Fig. 6-c, d) reduces the size of the separation and shifts the separation point downstream. The two-suction jet configuration is visually indistinguishable from the full four jet result (Fig. 6-b). Interestingly, the blowing jets are not particularly effective by themselves (Fig. 6-e), however, when combined with the two suction jets, the location of the more forward blowing jet (blowing jet 2) is close to the point of separation with the near-tangential blowing accelerating the flow downstream, potentially keeping the flow attached a bit longer. The more tailward jet (blowing jet 1) is in the separation bubble and is also relatively tangential, presumably to counter the adverse flow of the re-circulation. Still, the migrating effects of these two jets appears to be fairly limited and appears to be weaker than the effect generated by the single blowing jet in the two jet simulation⁽⁴⁾.

The results from the EARND GA evolution are not as fit. The current evolution has done a poor job compared to the Continuous GA (Fig. 6). The maximum fitness value is only 2.12, still a 6% increase over the no jet baseline, but less than that of the Continuous GA. Table 3 presents the best configuration generated by the EARND GA, with clear differences in the placement of the first jet, the angles of both suction jets and one blowing jet, and the magnitude of the blowing in both cases.

Similar to the CGA analysis, Fig. 8 shows the streamline plots for the jets using the best configuration generated by the EARND GA. It is interesting to note that we have a smaller separation bubble (and a slightly higher fitness, Table 4) for the case with the suction jet 1 and 2 along with blowing jet 2 as compared to all the four jets on. A possible explanation for that is the fact the EARND GA selected a configuration in which it had a normal blowing jet and it is possible that it got stuck in that local minimum. Another reason for this failure is that with only 56 individuals per generation and 11 parameters, the degree of diversity in each generation may not be sufficient to overcome unfortunate random mutations and crossovers. The selection scheme of the Continuous GA, in which the best half of the previous generation is explicitly retained, can mitigate against dramatic fitness declines. On the other hand, the techniques designed to drive convergence in the EARND GA can keep the evolution heading towards a less optimal configuration region once it gets started down the wrong path. As with any stochastic approach, it is quite possible that a repeat of the EARND GA evolution would randomly stumble onto a better path and yield a better result, but the outcomes of the two completed evolutions and the algorithm details suggest that the Continuous GA may be the more robust approach for this type of flow control problem.

The failure of the EARND GA to best situate the suction jets appears indirectly to have caused the blowing jets to achieve a greater degree of convergence than in the CGA evolution. As an experiment, therefore, the suction jets for the CGA best fitness configuration have been combined with the EARND GA best configuration blowing jets/ The resultant fitness is the highest of all (Table 4, last line), which suggests that the optimum blowing configuration may be better attained from a simulation with further reduced amplitude on the suction jets.

IV. Unsteady flow control simulation

Most active flow control techniques are not steady, but rather rely on unsteady means to control separation. Proper unsteady simulation of flow is generally more time consuming than steady simulations and the fitness evaluation of varying quantities present additional challenges to a GA-CFD simulation.

Synthetic jets have emerged as a promising approach to active flow control due to their high efficiency to cost ratio. The authors are in the process of setting up an unsteady GA-CFD system with the goal of optimizing the location, amplitude, angle and the frequency of synthetic jets. Experiments by Amitay et al⁽⁸⁾, Smith et al⁽⁹⁾ and Honohan et al⁽¹⁰⁾ and simulations of Vaddillo and Agarwal⁽¹¹⁾ and Sang Hoon Kim and Chongam Kim⁽¹²⁾ are being used to create realistic jet parameter ranges including mass flux and frequency.

The grid setup for the unsteady case is similar to the steady case with minor changes. The grid spacing of the top section (5% c to 80% c) of the airfoil where we typically place the jets is reduced from 0.001 to 0.0003 to accommodate the synthetic jets of relatively smaller jet width (0.03% c). This change increases the number of grid points by about 106,000 as compared to the steady jet case. CFD code (GHOST) is being used for this simulation, with appropriate changes to handle the unsteady flow.

V. Conclusions and future work

The optimum parameters for the steady four-jet (two-suction and two-blowing) are evaluated and presented. The jet setup considerably reduces separation and a significant increase in lift and noticeable decrease in drag is achieved. Also, it is shown that the CGA performs better than the EARND GA for this particular setup.

Basic setup of the unsteady synthetic jet control system is ready and initial test runs of the GA-CFD system are underway.

References

1. Gonzalez, L.F., E.J. Whitney, K. Srinivas, and J. Periaux, "Optimum Multidisciplinary and Multi-Objective Wing Design in CFD Using Evolutionary Techniques", *International Conference on Computational Fluid Dynamics 3*, Toronto, Canada, July 2004.
2. Mengistu, T. and Ghaly, W., "Aerodynamic Design of Transonic Cascade Using Parallel Computations of Global Optimizers and Artificial Neural Networks," *Proceedings of International Conference on Computational Fluid Dynamics 3*, Toronto, July, 12-14 2004.
3. Huang, L., Huang, P.G., LeBeau, R.P., and Hauser, Th., "Optimization of Blowing and Suction Control on NACA 0012 Airfoil Using a Genetic Algorithm", AIAA-2004-0423, 2004.
4. Huang, L., LeBeau, R.P., and Hauser, Th., "Application of Genetic Algorithm to Two-Jet Control System on NACA 0012 Airfoil", *Proceedings of the International Conference on Computational Fluid Dynamics 3*, Toronto, Canada, July 12-14, 2004.
5. R.L. Haupt and S.E. Haupt. *Practical Genetic Algorithms*. John Wiley and Sons, 2004.
6. Huang, L., Huang, P.G., LeBeau, R.P., Hauser, Th., "Numerical Study of Blowing and Suction Control Mechanism on NACA0012 Airfoil", *Journal of Aircraft*, Vol. 41, 2004, pp. 1005-1013.
7. Dannenberg, R.E. and Weiberg, J.A., "Section Characteristics of A 10.5-Percent Thick Airfoil With Area Suction As Affected By Chordwise Distribution Of Permeability", NASA Technical Note 2847, Ames Aeronautical Laboratory, Moffett Field, CA, Dec. 1952.
8. LeBeau, R.P., Beliganur, N and Hauser, Th., "Flow Control Optimization Using Neural Networks and Genetic Algorithms", *The Fourth International Conference on Computational Fluid Dynamics*, Ghent, Belgium, July 10-14, 2006. M. Amitay, V. Kibens, D. Parekh, and A. Glezer, "The Dynamics of Flow Reattachment over a Thick Airfoil Controlled by Synthetic Jet Actuators," AIAA Paper 99-1001, 37th AIAA Aerospace Sciences
9. D.R. Smith, M. Amitay, V. Kibens, D. Parekh, and A. Glezer, "Modification of Lifting Body Aerodynamics using Synthetic Jet Actuators," AIAA Paper 98-0209, 1998.
10. A.M. Honohan, M. Amitay, and A. Glezer, "Aerodynamic Control using Synthetic Jets," AIAA Paper 2000-2401, FLUIDS 2000 Conference, Denver, CO, June 2000.
11. Vadillo, J and Agarwal, RK, "Numerical study of Transonic Drag Reduction for Flow Past Airfoils Using Active Flow Control", *The Fourth International Conference on Computational Fluid Dynamics*, Ghent, Belgium, July 10-14, 2006. Katam, V., R.P. LeBeau, and J.D. Jacob, "Simulation of Separation Control on a Morphing Airfoil with Conformal Camber", AIAA2005-4880, 35th AIAA Fluid Dynamics Conference and Exhibit, Toronto, Canada, June 2005.
12. Sang Hoon Kim and Chongam Kim, "Separation control on NACA23012 using synthetic jets", 3rd AIAA Flow Control Conference, 5-8 June 2006, San Francisco, CA.
13. LeBeau, R.P., Beliganur, N, D.G. Schauerhamer, and Th. Hauser, "Application of Genetic Algorithms to Complex Computational Fluid Dynamics Simulations", 45th AIAA Aerospace Sciences Meeting and Exhibit, 8 - 11 Jan 2007, Reno, NV.

L_{s1}	θ_1	L_{b1}	θ_b1	A_{b1}	L_{s2}	θ_2	A_{s2}	L_{b2}	θ_b2	A_{b2}	C_l	C_d	Fit
0.05	84.377	0.7149	26.19	0.0928	0.0941	-2.289	0.0206	0.5218	0.597	0.0423	0.9961	0.14966	2.19098

Table – 1: Optimum parameters generated by CGA

CGA			
Configuration	C_l	C_d	Fitness
Baseline - no jets	0.891779	0.161013	2.000000
All four jets	0.996150	0.149930	2.190980
Suction Jet 1	0.958556	0.154350	2.118047
Suction Jet1 and 2	1.000812	0.151090	2.187939
Blowing Jet 1 and 2	0.888843	0.160040	2.002786
Suction Jet 1 and 2 with Blowing Jet 2	0.995930	0.150040	2.189922

Table – 2: Jet configuration using best fit data from CGA

L_{s1}	θ_{s1}	L_{b1}	θ_{b1}	A_{b1}	L_{s2}	θ_{s2}	A_{s2}	L_{b2}	θ_{b2}	A_{b2}	C_l	C_d	Fit
0.05	-90.00	0.8.00	90.00	0.1414	0.22	0.00	0.0212	0.6187	45.00	0.1.00	0.9252	0.14836	2.12283

Table – 3: Optimum parameters generated by EARND GA

EARND			
Configuration	C_l	C_d	Fitness
Baseline - no jets (a)	0.891779	0.161013	2.000000
All four jets (b)	0.925268	0.148361	2.122830
Suction Jet 1 (c)	0.917910	0.146343	2.129546
Suction Jet 1 and 2 (d)	0.950070	0.151124	2.130798
Blowing Jet 1 and 2 (e)	0.857941	0.153055	2.014051
Suction Jet 1 and 2 with Blowing Jet 2 (f)	0.939402	0.149684	2.129088
Combination if CGA and EARND	0.967548	0.144794	2.196974

Table – 4: Jet configuration using best fit data from EARND GA

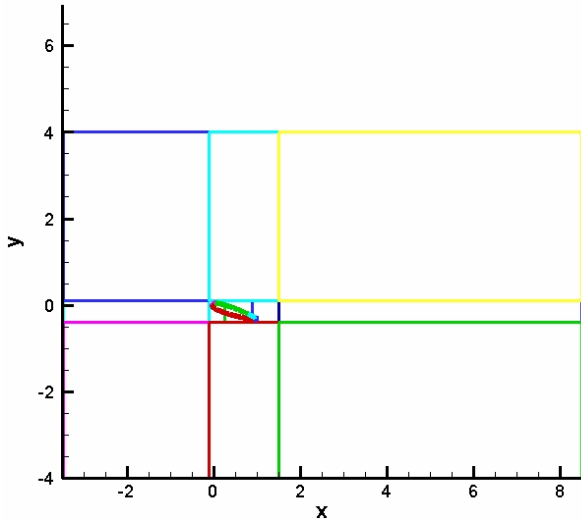


Figure 1: Multi-block grid arrangement for the base airfoil

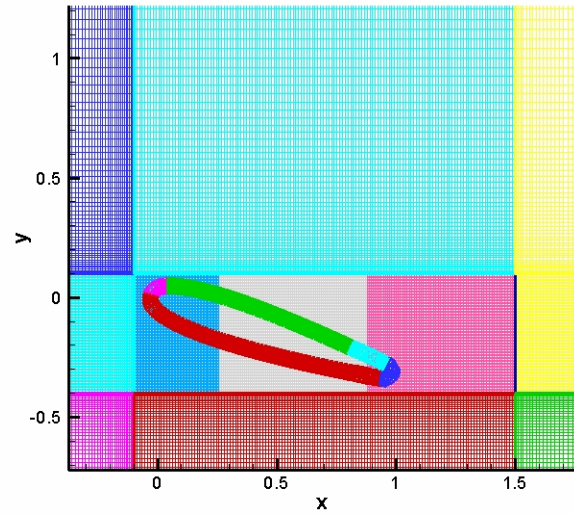


Figure 2: Five block airfoil grid and the background grids

NACA 0012 Airfoil Suction/Blowing Control

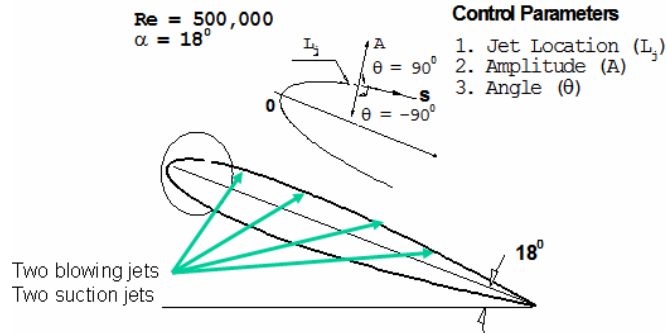


Figure 3: Schematic of the jet parameters for a single jet and the baseline flow conditions

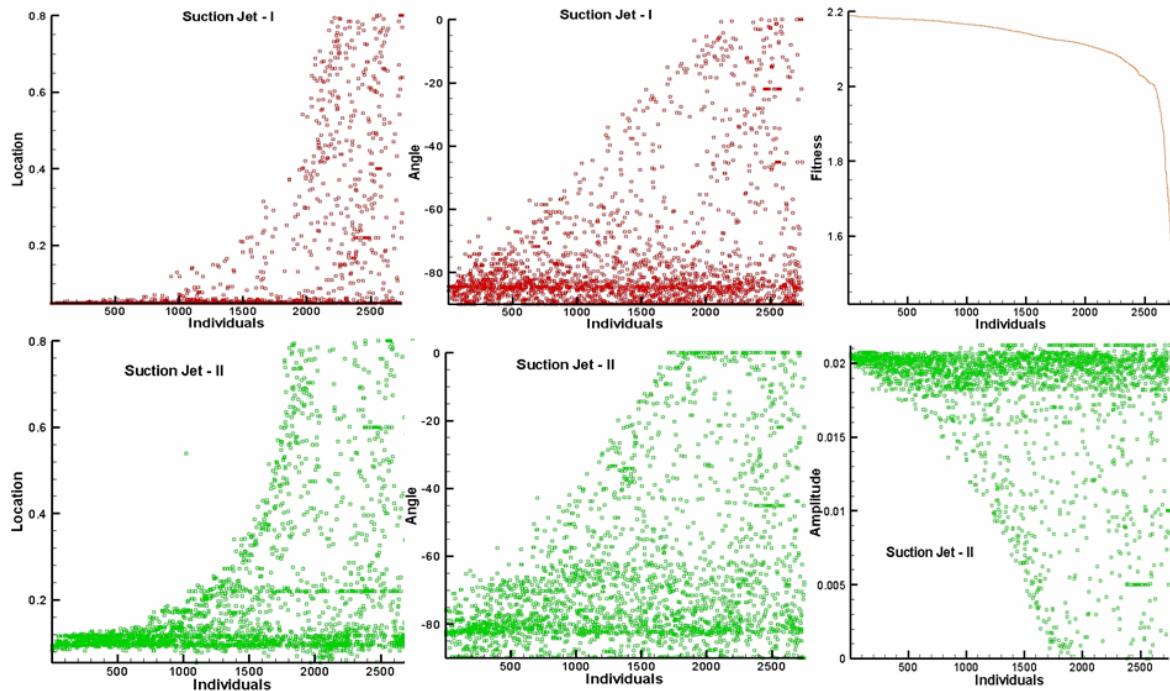


Figure 4-a

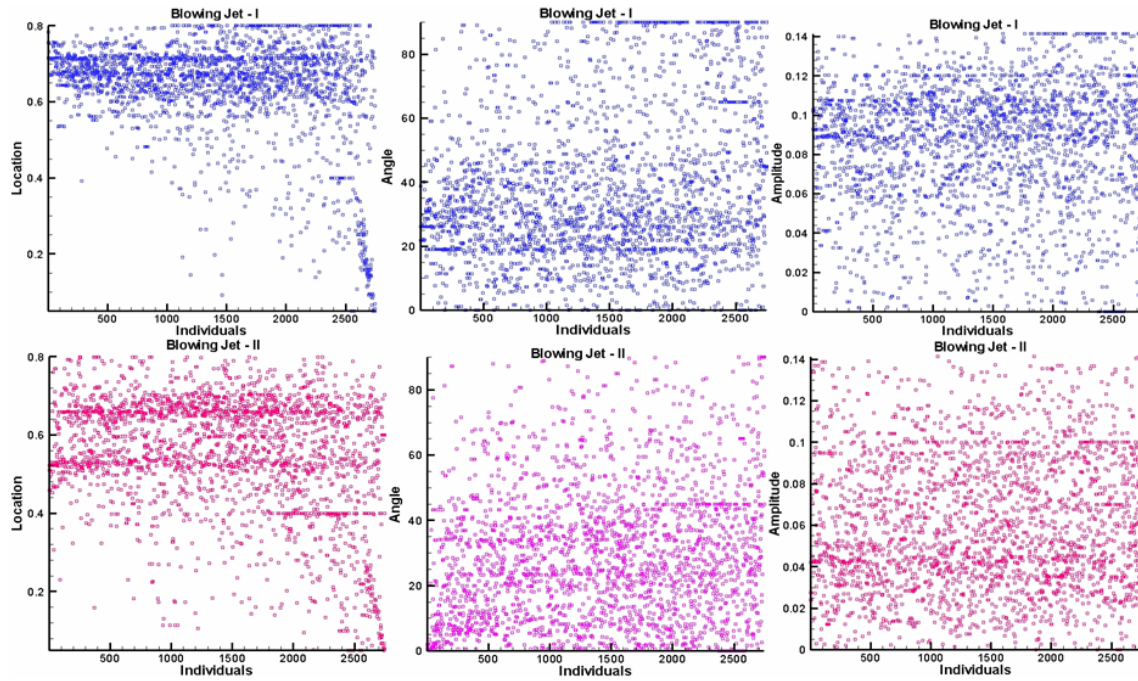


Figure 4-b

Figure 4: Overall fitness and distribution of the eleven parameters for all individuals (50 Generations) using CGA.

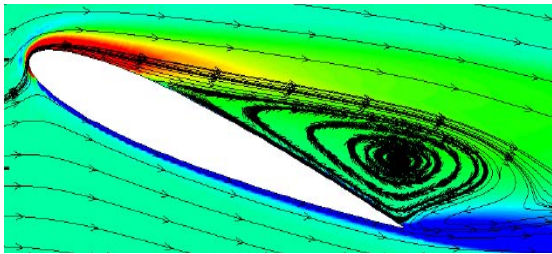


Figure 5-a: Velocity and streamlines plot of baseline

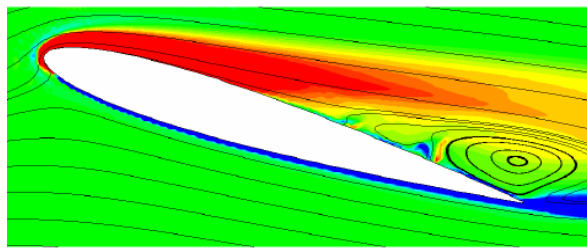


Figure 5-b: Velocity and streamlines using CGA

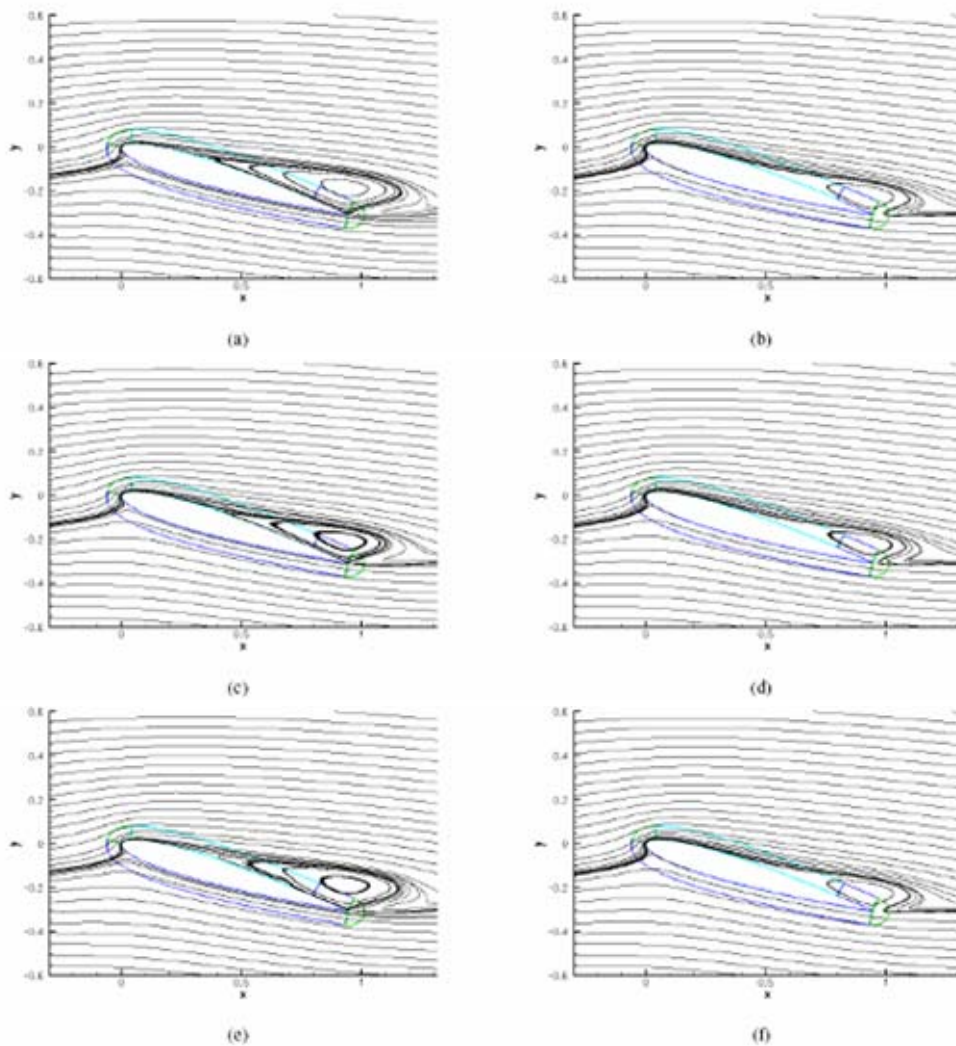


Figure 6: Streamlines for flow with various combinations of the four jets from the most fit configuration from CGA in Table 1: (a) no jets, (b) all four jets, (c) suction jet 1 only (d) suction jets 1 and 2, (e) blowing jets 1 and 2, (f) suction jets 1 and 2 and blowing jet 1

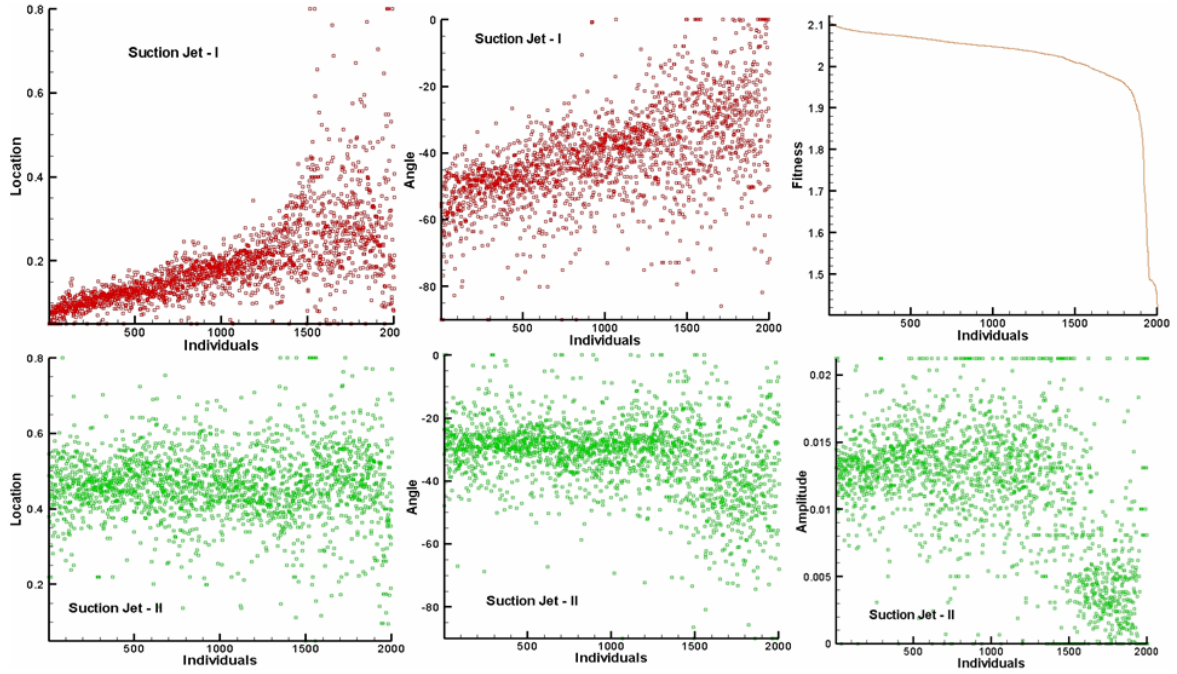


Figure 7-a

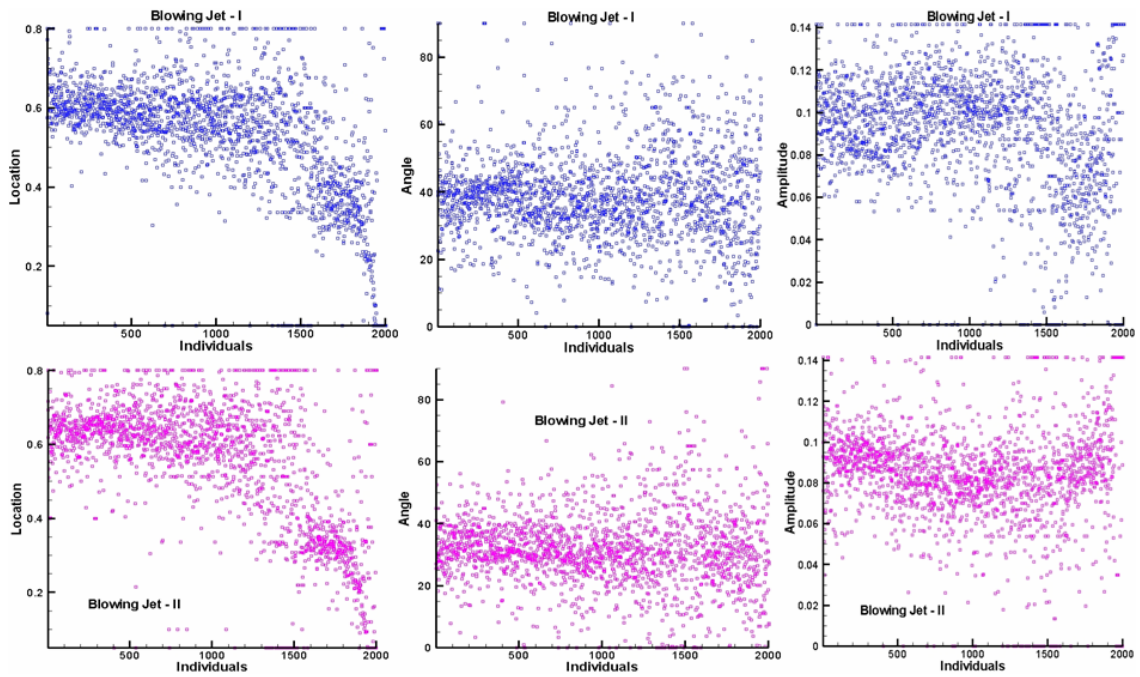


Figure 7-b

Figure 7: Overall fitness and distribution of the eleven parameters for all individuals (50 Generations) using EARND.

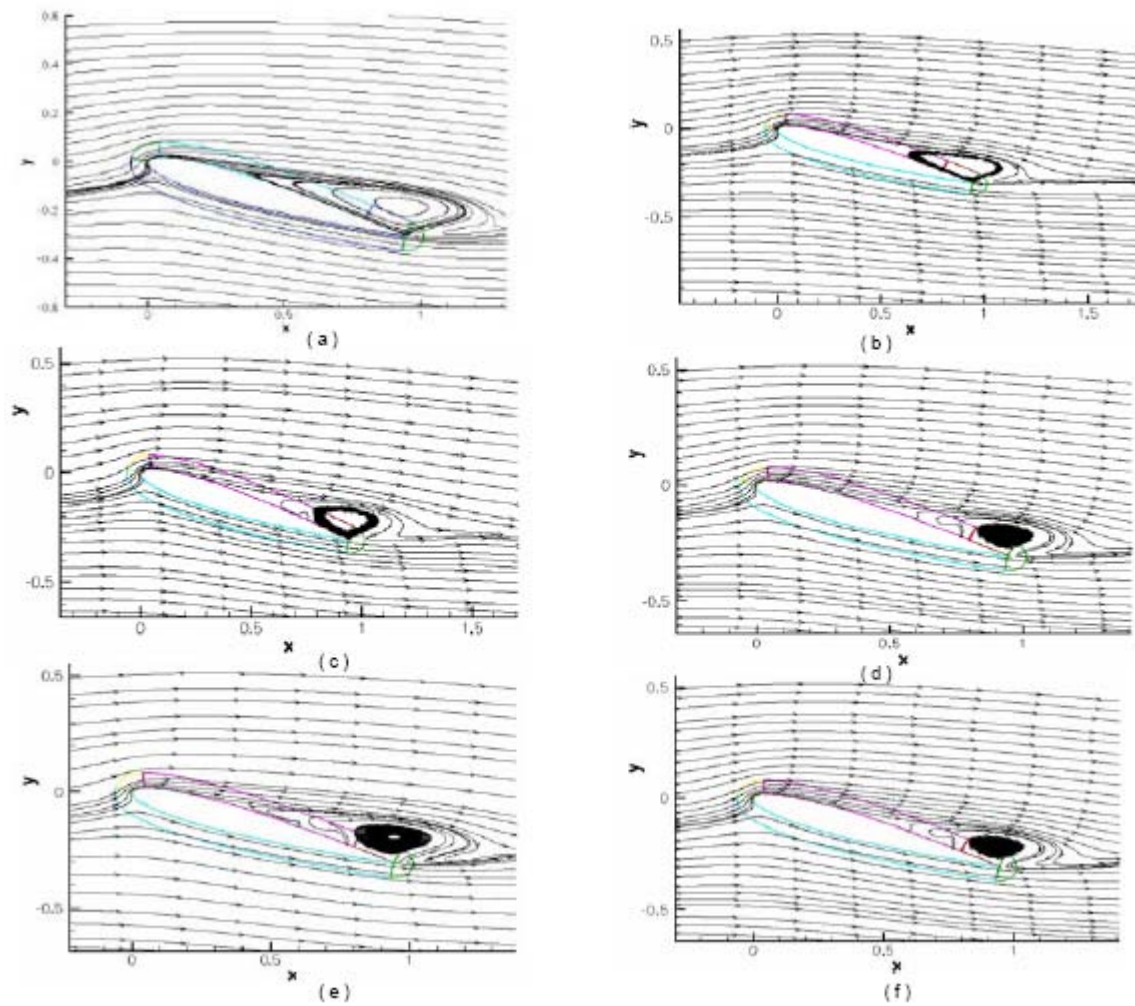


Figure 8: Streamlines for flow with various combinations of the four jets from the most fit configuration from EARND GA in Table 2: (a) no jets, (b) all four jets, (c) suction jet 1 only (d) suction jets 1 and 2, (e) blowing jets 1 and 2, (f) suction jets 1 and 2 and blowing jet 1